



ARTICLE

The Kalman Filter Design for MJS in Power System Based on Derandomization Technique

Quan Li^{1,*} and Ziheng Zhou²

¹State Grid Zhejiang Electric Power Corporation Ltd., Taizhou Power Supply Company, Taizhou, 317101, China

²College of Intelligent Science and Control Engineering, Jinling Institute of Technology, Nanjing, 211199, China

*Corresponding Author: Quan Li. Email: huaguoxiang141@163.com

Received: 09 June 2025; Accepted: 13 August 2025; Published: 27 November 2025

ABSTRACT: This study considers the state estimation problem of the circuit breakers (CBs), solving for random abrupt changes that occurred in power systems. With the abrupt changes randomly occurring, it is represented in a Markov chain, and then the CBs can be considered as a Markov jump system (MJS). In these MJSs, the transition probabilities are obtained from historical statistical data of the random abrupt changes when the faults occurred. Considering that the traditional Kalman filter (KF) frameworks based on MJS only depend on the subsystem of MJS, but neglect the stochastic jump between different subsystems. This study utilized the derandomization technique which transforms the stochastic MJS to a deterministic system to introduce the stochastic mode jumping in MJS, in which the state is still in the same norm, and the Lyapunov function is derived to show the stability condition of the systems, which proved that the transformed deterministic system is more conservative than the original MJS mathematically. After that, the Kalman filter algorithm is designed for estimating the state of the CBs depending on the transformed deterministic system. With the help of the Kalman filter, the estimation performance is derived by the recursive state estimation algorithm for the CBs. Furthermore, a single machine infinite-bus (SMIB) power system and a three-bus large scale system are proposed as practical examples to validate the effectiveness of the proposed algorithm.

KEYWORDS: Markov jump system (MJS); circuit breaker (CB); Kalman filter; derandomization technique; power system; mode transition

1 Introduction

Over the past several decades, power systems have undergone substantial advancements and have garnered increasing attention from worldwide researchers. This growing interest is primarily attributed to the pivotal role that power systems play in a broad spectrum of industrial applications [1,2]. As modern society becomes increasingly reliant on electricity, ensuring the reliability, efficiency, and resilience of power systems has emerged as a critical engineering challenge. Power systems are inherently complex, characterized by nonlinear dynamic behavior and susceptibility to low-frequency oscillations. These oscillations are not merely theoretical constructs but constitute essential dynamic features that significantly influence the overall stability of the power grid. They typically arise from the interactions among various system components, including synchronous generators, transmission networks, and time-varying load dynamics. A comprehensive understanding and effective mitigation of such oscillatory behaviors are therefore indispensable for maintaining secure and stable system operation and preventing potential instability or cascading failures.



Efficient energy conversion and delivery across the different layers of the power infrastructure are crucial for minimizing transmission losses and ensuring a high-quality power supply to end-users. The integration of renewable energy sources introduces additional complexity due to their variable and intermittent nature, necessitating advanced control strategies and real-time balancing mechanisms to maintain equilibrium between supply and demand [3]. Furthermore, the concept of energy storage has gained increasing prominence in the context of modern power systems, offering viable solutions to address temporal mismatches between energy production and consumption. Effective energy management is also intrinsically linked to power quality, which encompasses parameters such as voltage sags, harmonics, and frequency deviations. Maintaining acceptable power quality levels is essential for safeguarding sensitive equipment and ensuring the reliable and uninterrupted operation of both residential and industrial loads.

Consequently, a holistic investigation of power systems must encompass not only dynamic behaviors such as low-frequency oscillations, but also broader aspects related to energy flow, conversion efficiency, and long-term sustainability. Understanding and optimizing the interplay between system dynamics and energy management strategies is vital for the development of resilient, intelligent, and adaptive power grids capable of meeting the evolving energy demands of future societies. Neglecting these oscillations can result in severe consequences. It may compromise the stability of the entire power system, leading to increased transmission losses and reduced transmission line capacities. These issues result in higher operational costs and diminished system efficiency. Moreover, the quality of power supplied to end-users can be significantly degraded, affecting sensitive electronic equipment and industrial processes. Consequently, addressing and mitigating these oscillations is essential for ensuring reliable and high-quality power delivery [4]. In recent years, the power area has introduced several novel techniques, such as the power system stabilizers (PSSs) [5], the high voltage direct current (HVDC) [6] and the static voltage condenser (SVC) [7], which decrease the influence of the oscillations. Throughout the techniques mentioned above, the PSSs is one of the most efficient and commonly used methods in recent years according to the conventional structure in the practical industrial field [8,9]. Even if nonlinear behavior occurred in the power system, the PSSs is a traditional control technique which is designed depending on the linearized power system model in assorted working conditions [10].

Considering that the abrupt changes usually occurred in the actual power system, which is one of the key difficulties, there are many reasons that result in such a phenomenon, for example, component repairs [11], subsystem connection changes [12] and environmental disturbance exist [13]. To solve such difficulty, the power system treats these abrupt changes as a Markov chain [14–16], in which modes may jump to each other stochastically within a finite set at any time and there is no relationship between the stochastic jumping at different times. In general, such a class of systems with abrupt changes obeying a Markov chain is represented as a Markov jump system (MJS) commonly, and the finite modes are the subsystems in MJS. In the last decade, numerous researchers have focused on the analysis of MJSs, such as Kuppasamy et al., who studied the asynchronous controller to solve the stabilization problem of power systems with random abrupt changes in 2021 [16]. In 2024, Bahmani utilized a non-stationary discrete Markov model to provide a precise and valuable understanding of the constantly evolving and time-dependent nature of the power network [14].

Tracking the state of the power system makes great sense because the evolution of the power system will be determined clearly, and a certain controller can be activated. Kalman filter (KF) is one of the most common state estimation technique, which track the state by weighted combining the model evaluation and the measurement. However, the system modes are unable to be derived online with the stochastic jumping among different subsystems. Therefore, there are some difficulties in applying the Kalman filter algorithm to the MJSs. In this scenario, Borisov et al. devoted themselves to the optimal state filtering of the finite-state Markov jump processes with given indirect continuous-time observations corrupted by Wiener noise

in 2020 [17]. Zhang et al. designed a mode based Kalman filter for the MJSs with time correlated mode mismatch errors in 2021 [18]. In 2023, Costa et al. considered the finite horizon filtering problem of discrete-time Markov jump systems (MJS) satisfying some general nonlinear conditions [19].

However, most of the existing results are based on individual subsystems of the Markovian Jump System (MJS), while neglecting the stochastic transitions among different subsystems. In other words, the inherent randomness in mode jumping within MJSs is not adequately considered, which constitutes a significant limitation of these approaches, especially when applied to realistic MJS models. Generally, the Kalman filter (KF) framework based on subsystems of MJS requires prior knowledge of the current system mode before the recursive estimation process can be carried out. However, acquiring the exact mode information in practical MJSs is often either unavailable or computationally expensive, which poses a major challenge in the design of Kalman filters for such systems. To address this issue and develop an effective Kalman filtering algorithm for MJSs with stochastic mode transitions, a derandomization technique has been proposed [20,21]. This technique transforms the stochastic MJS into an equivalent deterministic system, in which the random mode transitions are embedded as part of the system dynamics. As a result, the Kalman filter can be directly applied to the transformed system, where the state maintains the same norm as that of the original MJS. This ensures that the estimation obtained from the transformed system is equivalent to that of the original MJS.

Moreover, the requirement for real-time mode determination in MJSs is effectively eliminated in the transformed deterministic framework. The stochastic mode jumping behavior is inherently incorporated into the estimation process through the system transformation. In addition, the performance of the Kalman filter is evaluated, demonstrating the effectiveness of the proposed approach and contributing to the advancement of Kalman filter design for MJSs.

The rest of this paper is organized as follows: In Section 2, the descriptions of power systems are provided, which are modeled in MJS and the derandomization technique is given, which transforms the discrete-time MJS to a deterministic system. In Section 3, the Kalman filter design based on the transformed deterministic system is presented. Then, the practical application of circuit breakers (CBs) exhibits the validity of the proposed technique in Section 4. The conclusion is given in Section 5.

Notations: R^n is the n -dimensional Euclidean space and $R^{m \times n}$ is the matrix with the dimension $m \times n$, respectively. $Diag\{A_1, A_2, \dots\}$ is specified as the block diagonal matrix. $A \otimes B$ is the Kronecker product of matrices A and B .

2 Materials and Methods

In this section, the detail of the Circuit Breakers working process is shown in Fig. 1 at first. In this figure, no matter the transient strikes or permanent faults occur online, the circuit breakers (CBs) isolate the line immediately to protect the whole power system network. After a while, the CBs will attempt to auto-reclose, which tests whether the power system would work normally. In common sense, the transient fault occurred due to the strike will end in several seconds. However, if the faults are unable to elapse transiently, which means the permanent fault occurs on line, then emergency repairs are needed.

To show the practical circuit breaker in a switch cabinet in a power system much more clearly, the structure can be modeled as a single-machine connected to an infinite-bus (SMIB) with typical circuit components [22]. The machine is equipped with a thyristor exciter and the SMIB is represented by the Thevenin equivalent of a large power system network. Considering that simultaneous faults occurring on both lines are extremely rare in practice, this paper assumed that only one line has malfunctioned probably, in which the faults, usually known as the stream of lightning strikes at random time instants, are setting on line in this study. The structure of the SMIB subject to random faults is provided in Fig. 2.

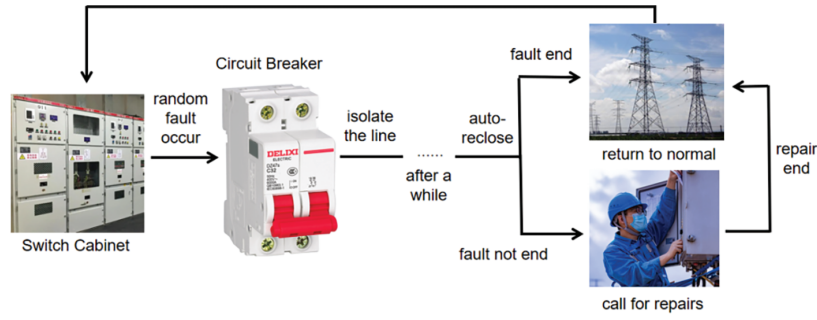


Figure 1: Working process of circuit breakers

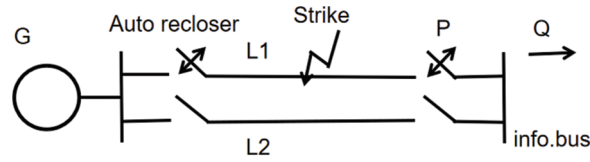


Figure 2: The structure of SMIB subject to random faults

With the relationship between the variables analyzed based on Thevenin's theorem, the nonlinear system model is proposed by the following differential equations [23].

$$\begin{cases} \dot{\delta} = \omega_0 \omega \\ \dot{\omega} = \frac{T_m - T_e}{M} \\ \dot{E}'_q = \frac{1}{T'_{d0}} \left(E_{fd} - \frac{x_d + x_q}{x'_d + x_q} E'_q + \frac{x_d + x'_d}{x'_d + x_e} V \cos \delta \right) \\ \dot{E}_{fd} = \frac{1}{T_E} (K_E E_{ref} - K_E V_t - E_{fd}) \end{cases} \quad (1)$$

where δ , ω and ω_0 represent the torque angle, angular velocity and synchronous speed of the generator, respectively. T_m , T_e and M denote the mechanical, electrical torques and the moments of inertia of the generator, respectively. E'_q , T'_{d0} and E_{fd} represent quadrature-axis voltage behind transient reactance, direct-axis open circuit field time constant and field voltage, respectively. x_d , x'_d and x_q denote direct-axis transient reactance, direct and quadrature-axes synchronous reactance of the generator, respectively. Moreover, x_e represents transmission line reactance; T_E and K_E are time constant and exciter gain; E_{ref} and V_t specify the infinite bus and terminal voltages, respectively.

Then we set the state vector as $x = [\delta \quad \omega \quad E'_q \quad E_{fd}]^T$, the differential equations in (1) can be linearized as the following state space model:

$$\dot{x} = \begin{bmatrix} 0 & \omega_0 & 0 & 0 \\ -\frac{k_1}{M} & 0 & -\frac{k_2}{M} & 0 \\ -\frac{k_4}{T'_{d0}} & 0 & -\frac{1}{k_3 T'_{d0}} & -\frac{1}{T'_{d0}} \\ -\frac{k_5 K_E}{T_E} & 0 & -\frac{k_6 K_E}{T_E} & -\frac{1}{T_E} \end{bmatrix} x \quad (2)$$

which can be simply written as $\dot{x} = Ax$, where $A \in R^{4 \times 4}$. More specifically, the analytic expressions for the parameters k_1, \dots, k_6 are functions of the loading conditions P and Q for different operating ranges shown in Table 1.

Table 1: Loading conditions P and Q

Loading condition	P (pu)	Q (pu)
Heavy	1	0.5
Nominal	0.7	0.3
Light	0.4	0.1

As mentioned previously, the Markov chain is utilized to analyze the random abrupt topology changes of the subsystem structure in power systems. Considering that the random abrupt changes and the shift operator of Eq. (2) can be discretized as a discrete-time Markov jump system (MJS), and the parameters of the MJS are identified depending on the mechanistic models and historical data by the least squares method. Then the MJS state evaluation model is written as follows:

$$x(k+1) = A(\theta_k)x(k) + B(\theta_k)w(k) \quad (3)$$

where k is the time moment, θ_k is the Markov chain taking value from a finite set $\theta_k \in M \{1, 2, \dots, m\}$ and the mode transition probability matrix Π , the items of which are represented as $\pi_{ij} = \Pi(\theta_k = i | \theta_{k+1} = j)$, which denotes the transition probability from mode i at time k to mode j at time $k+1$ and satisfies $\sum_{j=1}^m \pi_{ij} = 1$ when $i, j \in M$. $A(\theta_k)$ and $B(\theta_k)$ are constant matrices with appropriate dimensions, which are simplified as A_i and B_i , where $A(\theta_k)$ is matrix A obtained from Eq. (2) depending on different loading conditions.

Considering that the system is modeled in MJS, the transition probability π_{ij} in power systems can be analyzed as follows. It is widely known that the transient faults are utilized to be cleared by auto-reclosers in the power system, and the recloser will attempt several times to restore interlinks with set time delays once the faults occur. According to the historical statistics, there are 80% of the faults can be cleared after the first shot of CB reclosing, which is known as the transient faults. Only near 7% are unable to be cleared by the recloser attempts and the reclosing relay is locked. The probability of the transient fault and permanent fault transmission depends on the down and up mode according to the Markov chain in the power system, it can be obtained based on the historical statistical data from the power system, which has $\pi_{11} = 0.07$, $\pi_{12} = 0.93$, $\pi_{21} = 0.2$, and $\pi_{22} = 0.8$, as shown in Table 2.

Table 2: Transition probability of the recloser

Transmission line	Down	Up
Down	0.07	0.93
Up	0.2	0.8

Then the mode transition of up and down modes and the transition probability are proposed in Fig. 3.

Meanwhile, we consider the measurements of the MJSs (3) as follows:

$$y(k) = C(\theta_k)x(k) + D(\theta_k)v(k) \quad (4)$$

where $y(k) \in R^{n_y}$ is the noisy measured output, $v(k) \in R^{n_v}$ is the measurement noise.

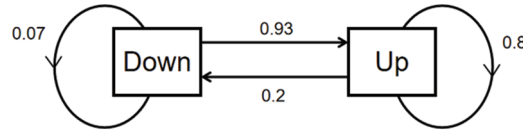


Figure 3: Transition of the MJSS modes depending on the line failure

The problem proposed in this paper can be formulated as estimating the discrete power system modeled as Eqs. (3) and (4) recursively. In MJSSs, the stochastic mode jumping is the key problem for the recursive state estimation process. Considering the transition probability in MJSSs, one of the most widely accepted ideas is weighting the next moment mode based on the transition probability according to the mode in the current moment. Depending on this idea, the probable mean of the state is derived based on the weighted mode prediction. Considering that the weighted idea is able to transform the stochastic MJS to a deterministic one, this idea can be formulated as a derandomization technique. Therefore, to establish the recursive state estimation based on the power system with a stochastic jumping problem, the derandomization technique is proposed in the following.

Firstly, a Dirac function 1_A is defined as follows [21]:

$$1_A(\omega) = \begin{cases} 1 & \text{if } \omega \in A \\ 0 & \text{otherwise} \end{cases} \quad (5)$$

Then define:

$$q_i(k) = E \{ \|x(k)\| 1_{\{\theta_k=i\}}(\theta_k) \} \quad (6)$$

where $q_i(k)$ is inferred as the expectation of $x(k)$ according to the mathematical transformation in Eq. (6) with the help of the Dirac function.

Combining Eqs. (3) and (5) and considering the definition of the Dirac function 1_A , it has $1_{\{\theta_k=i\}}(\theta_k) \cdot 1_{\{\theta_k=i\}}(\theta_k) = 1_{\{\theta_k=i\}}(\theta_k)$ and $1_{\{\theta_k=i\}}(\theta_k) 1_{\{\theta_{k+1}=j\}}(\theta_{k+1}) = \pi_{ij}$ according to basic probability conception. Therefore, the state evolution of $q_i(k)$ in each subsystem can be obtained as follows:

$$\begin{aligned} q_j(k+1) &= \sum_{i=1}^m A_i x(k) 1_{\theta_k=i}(\theta_k) 1_{\theta_{k+1}=j}(\theta_{k+1}) \\ &= \sum_{i=1}^m \pi_{ij} A_i q_i(k) \end{aligned} \quad (7)$$

Then, define the extended state vector and the extended noise vector as: $S(k) = \{q_1^T(k), \dots, q_m^T(k)\}^T$, $w_m(k) = \{w^T(k), \dots, w^T(k)\}^T$ which has appropriate dimensions. Eqs. (3) and (6) can be combined and expressed as:

$$S(k+1) = A_t S(k) + B_t w_m(k) \quad (8)$$

where $A_t = (\Pi^T \otimes I_{n_x}) \cdot \text{diag}\{A_1, A_2, \dots, A_m\} \in R^{(n_x \times m) \times (n_x \times m)}$, $B_t = \text{diag}\{B_1, \dots, B_m\}$.

Till Eq. (8), the discrete MJS (3) with stochastic mode jumping is transformed to a deterministic system in Eq. (8), in which the state only evolves depending on moment k . Meanwhile, the state $x(k)$ in Eq. (3) and extended state $S(k)$ in Eq. (7) has the same norm according to the definition of extended state $S(k)$, which denotes that the recursive estimation of the extended state $S(k)$ is equivalent to the state estimation of $x(k)$ in Eq. (3).

Remark 1: With the help of the derandomization technique, the CBs modeled in MJS can be transformed to single mode system, and the extended state vector in the transformed system has the same expectation as the original MJS, the corresponding parameter of expectation is the mean and the state estimation is mean value estimation.

For better understanding, the Lyapunov function of these transformed systems based on the derandomization technique and the original MJS is proposed to verify the system stability as follows:

Lyapunov stability criterion for MJS: There exists a group of positive definite symmetric matrix $\exists P_i > 0$ for every subsystem $i = 1, \dots, m$ through the whole finite set in Markov chain, when the MJS has the following inequalities $A_i^T \sum_{j=1}^m \pi_{ij} P_j A_i - P_i < 0$ while $i = 1, \dots, m$, then the MJS is stable depending on the Lyapunov stability definition. For circuit breakers (CBs), this stability guarantee means: (1) Fault recovery: After clearing a transient fault, contactor oscillations decay exponentially; (2) Stress tolerance: Permanent fault modes won't cause runaway mechanical vibrations.

If all the inequalities above are listed in the inequality matrix, it can be formulated as:

$$\begin{bmatrix} A_1 & & \\ & \ddots & \\ & & A_m \end{bmatrix}^T \begin{bmatrix} \pi_{11}P_1 & \dots & \pi_{1m}P_m \\ \vdots & \ddots & \vdots \\ \pi_{m1}P_1 & \dots & \pi_{mm}P_m \end{bmatrix} \begin{bmatrix} A_1 & & \\ & \ddots & \\ & & A_m \end{bmatrix} - \begin{bmatrix} P_1 & & \\ & \ddots & \\ & & P_m \end{bmatrix} < 0 \quad (9)$$

Considering that all the diagonal elements in the above inequality matrix are $A_i^T \sum_{j=1}^m \pi_{ij} P_j A_i - P_i < 0$ with $i = 1, \dots, m$, the MJS Lyapunov stability condition can be written as such an inequality matrix.

Considering that the transition probability elements π_{ij} are scalars, the inequality matrix can be rewritten as:

$$\begin{bmatrix} A_1 & & \\ & \ddots & \\ & & A_m \end{bmatrix}^T \Pi \otimes I^{n_x} \begin{bmatrix} P_1 & & \\ & \ddots & \\ & & P_m \end{bmatrix} \begin{bmatrix} A_1 & & \\ & \ddots & \\ & & A_m \end{bmatrix} - \begin{bmatrix} P_1 & & \\ & \ddots & \\ & & P_m \end{bmatrix} < 0 \quad (10)$$

As commonly known that all the elements in the transition probability matrix $\pi_{ij} \in (0, 1)$, it has $\Pi - I < 0$. According to the constraints of Π , a more conservative inequality can be given as follows:

$$\begin{bmatrix} A_1 & & \\ & \ddots & \\ & & A_m \end{bmatrix}^T (\Pi \otimes I^{n_x})^T \begin{bmatrix} P_1 & & \\ & \ddots & \\ & & P_m \end{bmatrix} \Pi \otimes I^{n_x} \begin{bmatrix} A_1 & & \\ & \ddots & \\ & & A_m \end{bmatrix} - \begin{bmatrix} P_1 & & \\ & \ddots & \\ & & P_m \end{bmatrix} < 0 \quad (11)$$

After combining the multiplication of diagonal matrix $\text{diag}\{A_1, A_2, \dots, A_m\}$ and transition probability matrix Π , it has

$$\begin{bmatrix} \pi_{11}A_1 & & \pi_{1m}A_m \\ & \ddots & \\ \pi_{m1}A_1 & & \pi_{mm}A_m \end{bmatrix}^T \begin{bmatrix} P_1 & & \\ & \ddots & \\ & & P_m \end{bmatrix} \begin{bmatrix} \pi_{11}A_1 & & \pi_{1m}A_m \\ & \ddots & \\ \pi_{m1}A_1 & & \pi_{mm}A_m \end{bmatrix} - \begin{bmatrix} P_1 & & \\ & \ddots & \\ & & P_m \end{bmatrix} < 0 \quad (12)$$

We notice that all P_i are positive definite symmetric matrix, then the $\begin{bmatrix} P_1 & & \\ & \ddots & \\ & & P_m \end{bmatrix}$ is positive definite symmetric matrix as well.

Therefore, the stability inequality is proposed as: $\exists P = \begin{bmatrix} P_1 & & \\ & \ddots & \\ & & P_m \end{bmatrix} > 0, A_t^T P A_t - P < 0$, in which $A_t = \Pi \otimes I^{n_x} \text{diag}\{A_1, A_2, \dots, A_m\}$, which is the stability condition of Eq. (8) by Lyapunov function.

Above all, the Lyapunov function of both the original MJS (3) and the transformed deterministic system (8) is provided. The stability constraints in (8) are more conservative than (3), which implies that when the transformed deterministic system (8) is stable, the MJS (3) is stable as well, according to the Lyapunov function. This verifies the statement that the state has the same norm between the MJS (3) and the transformed deterministic system (8) after the utilization of the derandomization technique.

After the deterministic system is achieved, the Kalman filter is designed in the next section.

3 Main Results

In this section, the recursive state estimation based on the Kalman filter algorithm is derived depending on the transformed deterministic system derived in Eq. (13).

Then the explicit expression of the deterministic system is given as:

$$\begin{cases} S(k+1) = A_t S(k) + B_t w_m(k) \\ y_t(k) = C_t S(k) + D_t v_m(k) \end{cases} \quad (13)$$

where $y_t(k) = \{y^T(k), \dots, y^T(k)\}^T$ and $v_m(k) = \{v^T(k), \dots, v^T(k)\}^T$ have appropriate dimensions; w_m and v_m are the system noise and measurement noise in Gaussian with zero mean and covariance P_m and Q_m which have the same norm as P and Q according to the previous section in appropriate dimensions, respectively. $C_t = \text{diag}\{C_1, \dots, C_m\}$, $D_t = \text{diag}\{D_1, \dots, D_m\}$. The measurement output error is given by:

$$E_y(k) = y_t(k) - \hat{y}_t(k) \quad (14)$$

where $y_t(k)$ is the perturbed measurement and $\hat{y}_t(k)$ is the estimated measurement.

Then the Kalman filter based on the transformed deterministic system begins the recursive algorithm with the one step prior state prediction $S(k|k-1)$ and variance $P(k|k-1)$ as follows:

$$S(k|k-1) = A_t S(k-1|k-1) \quad (15)$$

$$P(k|k-1) = A_t P(k-1|k-1) A_t^T + Q \quad (16)$$

where $S(k|k-1)$ and $S(k-1|k-1)$ are the prior and posterior estimation of the state $S(k-1)$ at time $k-1$. Similarly, $P(k|k-1)$ and $P(k-1|k-1)$ are the prior and posterior variances.

Then the Kalman filter gain can be computed as follows:

$$K(k) = P(k|k-1) C_t^T (C_t P(k|k-1) C_t^T + Q)^{-1} \quad (17)$$

With the Kalman filter gain derived, the posterior state estimation is given in the following equation:

$$\begin{aligned} S(k|k) &= S(k|k-1) + K(k) E_y(k) \\ &= S(k|k-1) + K(k) (y_t(k) - C_t S(k|k-1)) \end{aligned} \quad (18)$$

Meanwhile, the posterior of the covariance is:

$$P(k|k) = (I - K(k) C_t) P(k|k-1) \quad (19)$$

Above all, the recursive state estimation result based on the MJS model of CBs is proposed as Algorithm 1 [20] follows:

Algorithm 1: KF based on derandomization technique

Input: CBs parameters based on MJS model $A_i, B_i, B_{wi}, C_i, D_i$, transition probability matrix Π

Initialize: initial state $x(0)$, initial mode $m(0)$, initial error covariance $P(0), Q(0)$

Model Transform: transform MJS model to deterministic system, in which the transformed state is $S(0)$ parameters are $A_{tp}, B_{tp}, B_{wtp}, C_{tp}, D_{tp}$ by the Eqs. (2)–(8)

for time = 1 to k , **do**

figure out Kalman gain $K(\text{time})$,

estimate the posterior state result $S(\text{time})$ Eqs. (15)–(19),

end for

Considering the transformed large-scale system, the key difference is the multiplicatively increasing dimension resulting from the Kronecker product, which has heavier computation complexity in the recursive estimation process, especially figuring out the Kalman gain with the high dimension matrix inverse in Eq. (17).

After the algorithm's proceedings are provided, the estimation performance of the result is shown by the root mean square error (RMSE) as follows:

$$RMSE(k) = \sqrt{(|x(k)| - |S(k|k)|)^T (|x(k)| - |S(k|k)|)} \quad (20)$$

According to Eqs. (11)–(15), the optimal posterior recursive estimation result $S(k|k)$ can be obtained. The values of the filter gains are given as $K(k)$, which is updated based on the variance of the system noise and measuring noise. At the last step of each recursion in the KF algorithm, the estimation precision is demonstrated by the error variance $P(k|k)$, which is updated and decreased because more measurement information has been considered and the Kalman gain compensation $K(k)$ is corrected recursively. The whole state estimation process of the CBs in on-off switch cabinet is proposed in the next section. It is obvious that the system transformation has solved the stochastic mode jumping problem in the MJSs, then the recursive state estimation technique, the Kalman filter algorithm, is available to be utilized.

Considering the system transformation process, it is easy to understand that the transformed state $S(k)$ has the same norm as $x(k)$ when considering Eqs. (5) and (6). Beside the description of the proposed derandomization technique, it is noted that some existing results of MJS Kalman filter framework have emerged in the utilization of the expectation of the stochastic system mode for the recursive state estimation. The brief descriptions are shown in corollary 1 and 2 as follows. After the corollaries, a remark is proposed to show the comparison between the derandomization method and the existing techniques.

Corollary 1 (Expectation method): Based on the MJS (3), the related system parameters are presented as $A_t = \sum_{j=1}^m \pi_{ij} A_j$ and $C_t = \sum_{j=1}^m \pi_{ij} C_j$ if the mode of MJS is i in the previous moment $k-1$. The steps of the state estimation are the same as Eqs. (15)–(19).

Corollary 2 (Subsystem based method): Based on the MJS (3), the parameters of the recursive state estimation methods are based on the subsystem parameters A_i and C_i with the current mode and $\theta_k = i$ known. The steps of the state estimation are the same as Eqs. (15)–(19).

Remark 2: Compared to the derandomization technique, Corollary 1 and 2 using the expectation of the matrix A_i or the current mode of the MJS in the existing results still has some constraints. It is evident that if these expectation parameters can be figured out, the mode of the MJS in the previous moment $k-1$

should be known. This constraint is not always satisfied due to the heavy computational pressure during the estimation process in practical applications.

For better understanding, a theoretical comparison table of the proposed method and existing techniques is provided as follows in Table 3:

Table 3: Comparisons of different KF based on MJS

	Derandomization KF	Expectation KF	Robust KF
Computation pressure	$O((n_x \times m)^3)$	$O(n_x^3)$	$O(n_x^3)$
Mode dependence	No	Yes	Yes
Conservation	Same norm	equal	equal
Parameter requestion	same	same	same

With the existing study of the recursive estimation of MJS given in corollary 1 and 2, the comparison between the algorithms mentioned above is revealed by the performance index RMSE given in Section 4.

4 Experimental Validation and Discussion

In this section, the performance of the Kalman filter algorithm incorporating a derandomization technique is demonstrated through the CBs examples in a practical power system. A two mode, one bus single system and a three-bus large scale system are provided to demonstrate the proposed KF based on derandomization technique. This simulation highlights the effectiveness and superiority of the proposed approach.

All the power system models are implemented using Simulink in MATLAB R2022a. The two mode one bus system modeled in MJS is divided by the mode indication signal, as illustrated in Fig. 4. Then the state is proposed from the scope. The sampling interval is 1 s for each sample.

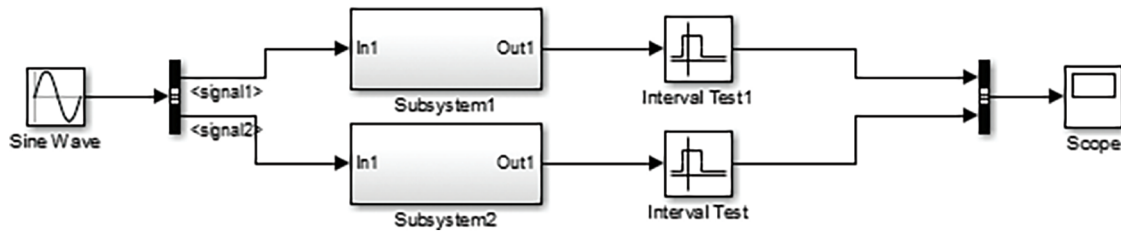


Figure 4: Simulink figure of the power system

In the following, the on-off switching behavior of circuit breakers (CBs) during line faults in a Markovian Jump System (MJS) with two modes, the occurrence of transient fault and permanent fault, is parameterized as follows [23]. All the parameters are derived from the historical statistical data according to the Thevenin's theorem in Eqs. (1)–(4) from the reference. The parameters of the considered system are represented as follows: the synchronous motor machine parameters: $x_d = 1.6$, $x'_d = 0.32$, $x_q = 1.55$, $\omega_0 = 50 \pi \text{ rad/s}$, $T'_{d0} = 6 \text{ s}$, and $M = 10$. The exciter-amplifier parameters: $K_E = 50$, $T_E = 0.05 \text{ s}$. Then the model system parameters are given as follows:

$$A_1 = \begin{bmatrix} 0.9833 & 9.368 & -0.01264 & -1.833 \times 10^{-5} \\ -0.003529 & -0.9833 & -0.002655 & -5.542 \times 10^{-6} \\ -0.00639 & -0.02936 & 0.955 & 0.003684 \\ -0.2623 & -1.253 & -11.31 & 0.5231 \end{bmatrix}$$

$$A_2 = \begin{bmatrix} 0.9866 & 9.378 & -0.008638 & -1.253 \times 10^{-5} \\ 0.002837 & 0.9866 & -0.001812 & -3.787 \times 10^{-6} \\ -0.002054 & -0.01243 & 0.9443 & 0.00367 \\ 0.6894 & 3.545 & -16.25 & 0.5118 \end{bmatrix}$$

$$B_1 = [-0.0001417 \quad -5.836 \times 10^{-5} \quad 0.06133 \quad 22.27]^T$$

$$B_2 = [-9.692 \times 10^{-5} \quad -3.99 \times 10^{-5} \quad 0.06123 \quad 22.15]^T$$

$$B_{w1} = B_{w2} = [0.3962 \quad -5.419 \quad 0.7924 \quad -2.5971]^T, C_1 = C_2 = [0 \quad 1 \quad 1 \quad 0]$$

$$D_1 = 0.57, D_2 = 0.893$$

As mentioned before, the goal of this paper is to design a recursive state estimation algorithm based on the derandomization technique. In this practical example, the Markov jump process has two modes and the transition probability matrix is given by $\Pi = \begin{bmatrix} 0.07 & 0.93 \\ 0.2 & 0.8 \end{bmatrix}$, which is derived in [Section 2](#). The stochastic mode jumping of MJS is achieved by the Matlab instruction “rand(0, 1)”, which generates uniform random numbers between [0, 1] and determines the system mode of MJS based on the corresponding interval of the transition probability matrix.

[Fig. 5](#) illustrates the stochastic transitions between the up and down modes exhibited by the system. To further elucidate the system's behavior, [Fig. 6](#) presents the open-loop variations of the four state variables during these mode transitions.

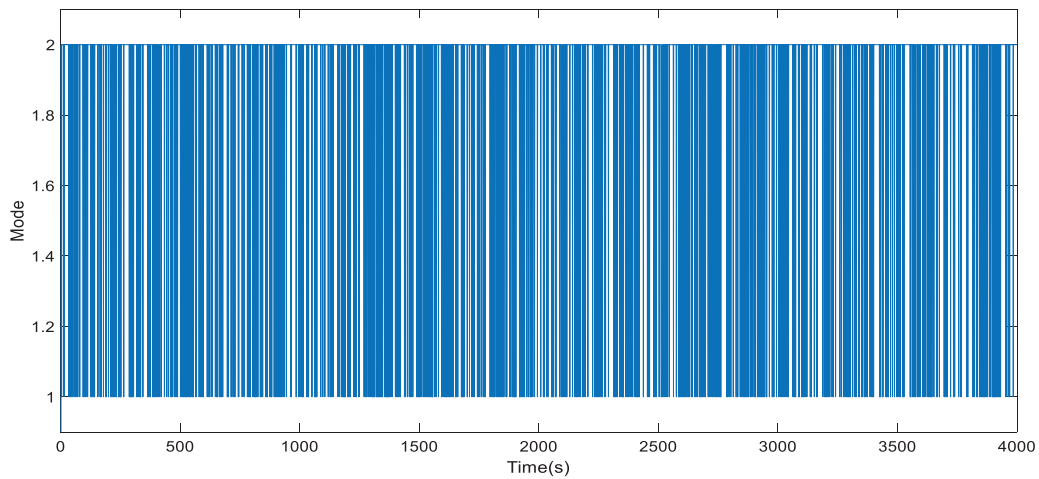


Figure 5: Mode transition between two modes

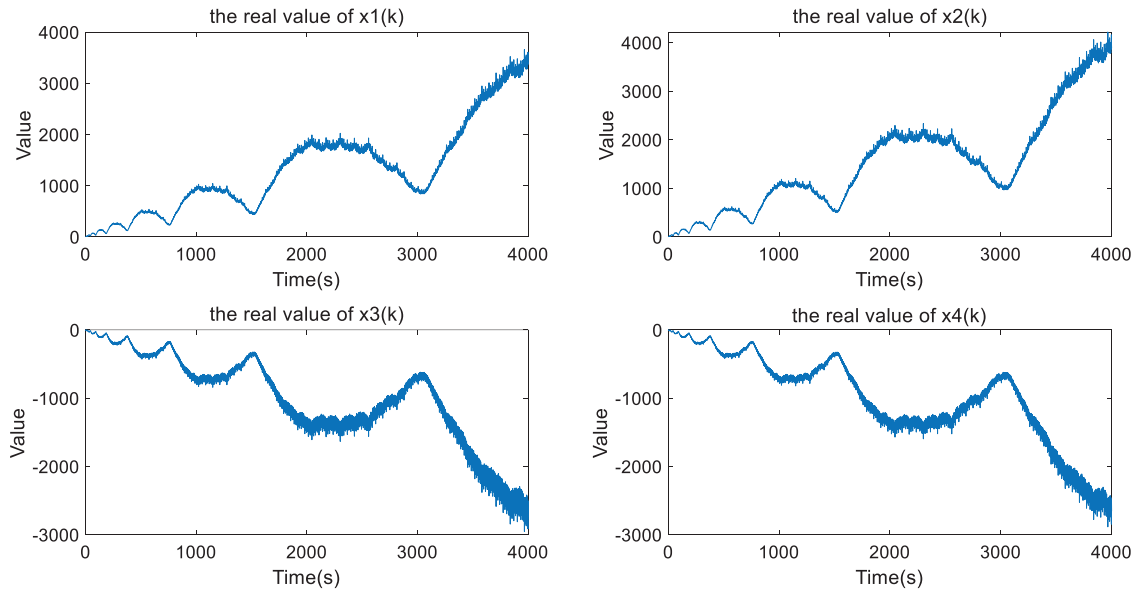


Figure 6: Open-loop state variation

To stabilize this open-loop system, a conservative solution based on feedback control is given by the linear matrix inequalities (LMI). Then the Kalman gain based on the stable system is given as follows:

$$K = \begin{bmatrix} 0.0038 & 0.0040 & 0.9960 & 0.8566 & 0 & 0 & 0 & 0 \\ 0 & 0 & 0 & 0 & 0.0025 & 0.0027 & 0.9972 & 0.8579 \end{bmatrix}^T$$

The Kalman gain of the proposed method is based on the extended batch of states, and it can be divided into two Kalman gains depending on each subsystem that:

$$K_1 = [0.0038 \quad 0.0040 \quad 0.9960 \quad 0.8566]^T$$

$$K_2 = [0.0025 \quad 0.0027 \quad 0.9972 \quad 0.8579]^T$$

With the mathematical proof that the transformed deterministic system is a more conservative system than the original MJS in the previous section, the Kalman gain is available for the two modes, the transient fault and the permanent fault. Furthermore, the stochastic mode switching is considered as well by such a technique.

Fig. 7 shows the estimation results and the real value of the recursive state estimation algorithm. To show the estimation performance, the RMSEs derived from Eq. (15) are given in Fig. 8. The stochastic mode transition of the Markov chain (θ_k), which is also known as the switching between loading conditions. Meanwhile, the RMSEs values and the 95% confidential interval are proposed in Tables 4 and 5, which directly demonstrate the advantages and effectiveness of the derandomization technique.

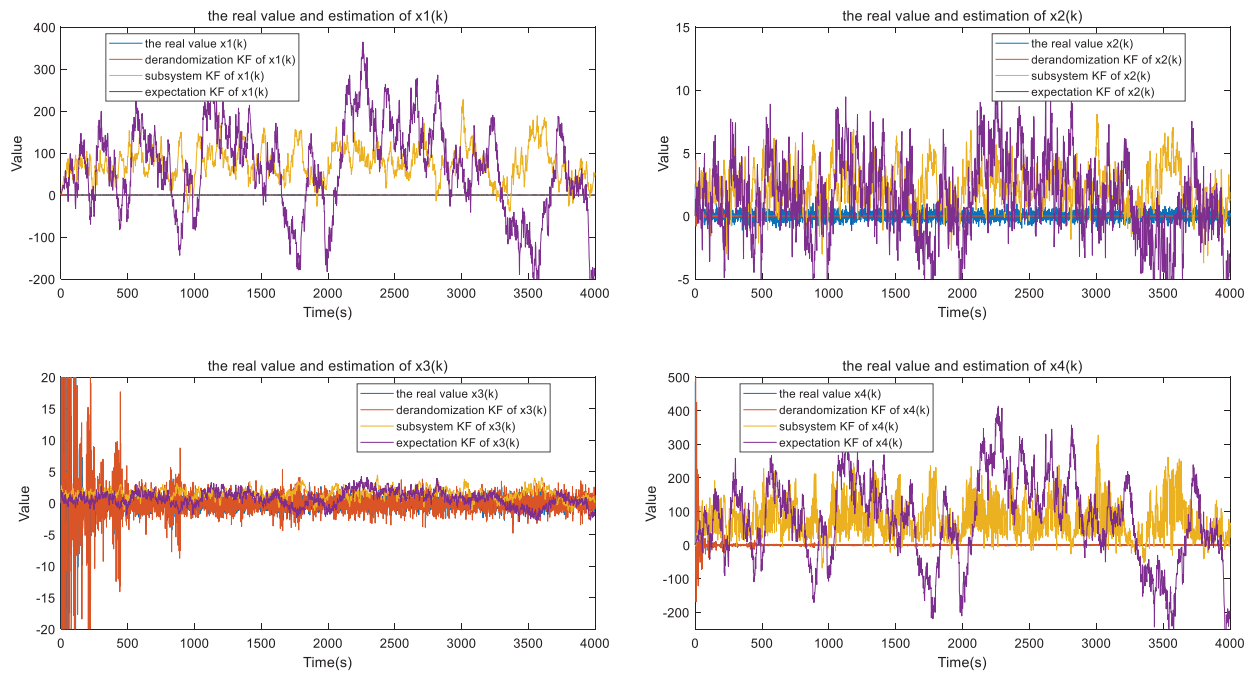


Figure 7: The estimation result and the real value of each state component

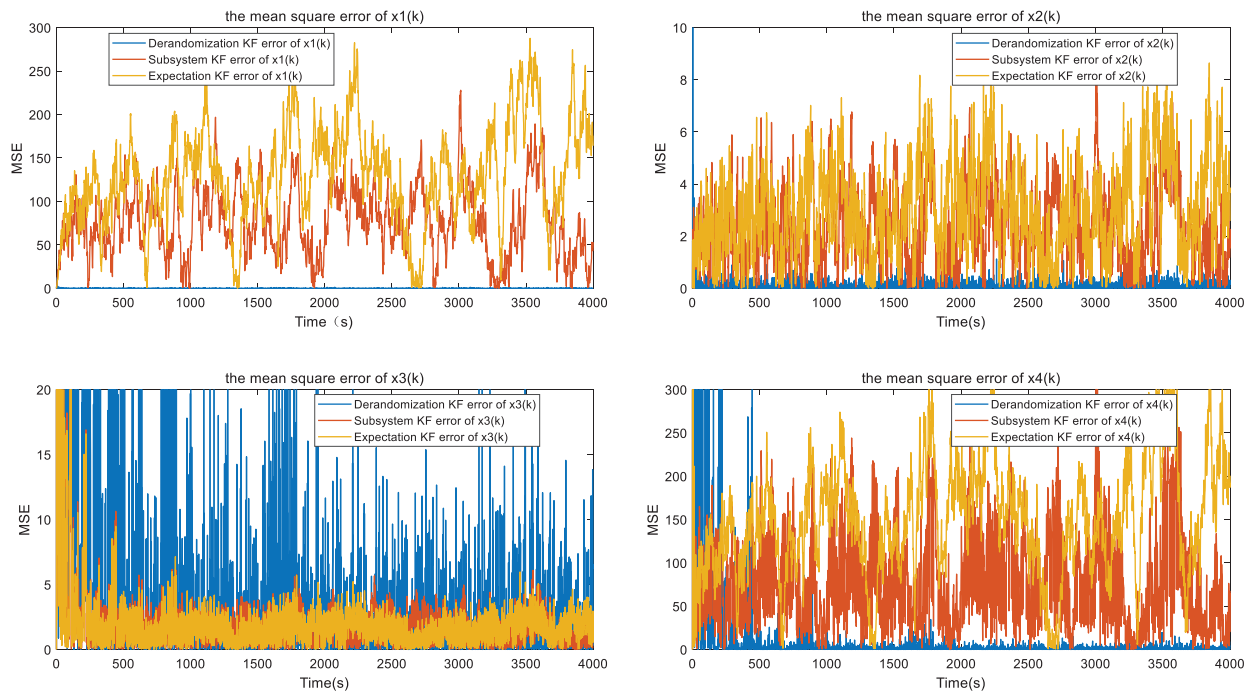


Figure 8: The RMSE of each state component in different KF algorithms

Table 4: RMSE of different state components based on different estimation technique

State component	Derandomization KF	Expectation KF	Robust KF
x_1	0.2618	8.3621	1.1268
x_2	0.2666	1.1189	1.3586
x_3	3.4102	0.8646	0.9515
x_4	2.9403	12.0001	9.1954

Table 5: 95% confidential interval of different state components based on different estimation technique

State component	Derandomization KF	Expectation KF	Robust KF
x_1	(78.0159, 78.0229)	(78.4575, 79.4840)	(78.6364, 79.2224)
x_2	(2.7044, 2.7127)	(2.6025, 2.7275)	(2.6823, 2.7395)
x_3	(1.9487, 1.9670)	(1.8929, 1.9820)	(2.0389, 2.0732)
x_4	(38.1696, 38.7582)	(38.7280, 39.9779)	(39.0928, 39.8751)

From the simulation results presented above, it is evident that the recursive state estimation algorithm for Markovian Jump Systems (MJSs) in power systems performs effectively when the derandomization technique is applied. This approach explicitly accounts for the stochastic mode transitions during the estimation process. By incorporating the randomness of mode jumping in the MJS modeling of circuit breakers (CBs), the proposed method achieves significantly lower root mean square error (RMSE) in state estimation compared to the expectation-based method in Corollary 1 and the robust method in Corollary 2.

Fig. 7 illustrates the true system states alongside the estimated values, while Fig. 8 presents the RMSEs of the aforementioned methods discussed in the previous section. To further demonstrate the estimation performance, Table 1 summarizes the RMSE values obtained from the estimation process. Compared to the existing results studied in 2023 [19], it is obvious that the derandomization technique has transformed the stochastic mode jumping in MJS to a deterministic system, which has the same norm as the original MJS. The existing KF framework mostly estimates the state based on each subsystem or the expectation of the weighted modes. Then, the MJS-KF based on the subsystem has not introduced the transition probability information. Especially, the transition probability affects the stability of the MJS, which is clearly proved in the Lyapunov stability constraints. Else, the estimation error of KF based on the expected weighted modes of MJS is obviously larger than the proposed technique due to the hybrid weighted mode information introduced. Besides, all these existing KF frameworks have the constraint that the current mode should be known. Nevertheless, the proposed MJS-KF based on the derandomization technique can begin the estimation process without the need for known current mode information.

Additionally, to compare this proposed method with recent advancements in MJS-based Kalman filtering, there is an expanded discussion. In [24], it analyzes the convergence characteristics of the factorial Kalman filter, which ensures that the Kalman gain converges at $t \rightarrow \infty$. Specifically, it provides sufficient convergence conditions for Kalman gain, but it is not suitable for the state estimation problem of the circuit breakers (CBs) solving random abrupt changes that occur in power systems. In [25], Bayesian deep learning and Kalman net are integrated to quantify uncertainty without additional domain knowledge by sampling prediction error covariance. However, it relies on many training data and GPU calculations, and its real-time performance is poor. The deterministic transformation in this paper only needs the historical transition probability, and the calculation time in the SMIB system is less, which is more suitable for online estimation

of the power system. Reference [26] proposes an improved maximum correlation entropy Kalman filter to enhance the robustness to non-Gaussian noise (such as impulsive noise) by introducing a weighted factor cost function. However, the method in [26] needs to manually adjust the kernel width parameter, which limits its generalization in the power system catastrophe scenario. In this paper, the solution of randomization depends on the historical statistical noise model. In the CB Gaussian noise scene studied in this paper, RMSE is equivalent to IMCKF, but the implementation is simpler. Furthermore, the Kalman filter Gaussian mixture model is presented in [27]. The Gaussian mixture model is used to approximate the fuzzy TDOA measurement and improve the accuracy of multi satellite positioning. However, the computational complexity increases exponentially with the number of mixed components, which makes it difficult to extend to large power grids. In this paper, the solution randomization compresses the multi-modal MJS into a single-mode system. In SMIB, only a single Kalman filter is needed, and the memory consumption is reduced.

Overall, the necessity and superiority of the derandomized MJS-based Kalman filter are clearly demonstrated based on the results shown in Figs. 7 and 8 and Tables 3 and 4, particularly when compared with existing Kalman filter algorithms designed for MJSs.

For better verification, a multi-machine case with 6-bus and 3-machine in the system is provided, and the structure is shown in Fig. 9 [22]. In this system, random faults occurred in lines 1–4 and 1–5, which are modeled as three subsystems in MJS. As listed in the reference, the critical parameters are proposed in Table 6.

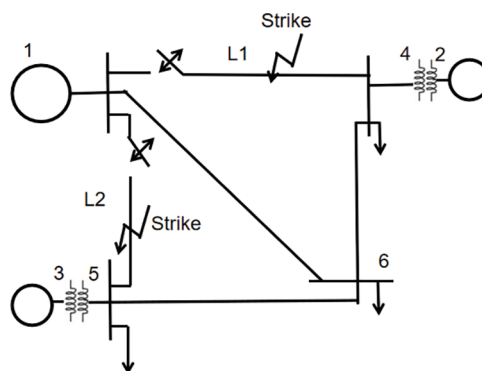


Figure 9: 6-buses and 3-machine system

Table 6: System data and nominal loading conditions

Bus number	1	2	3	4	5	6
Load, Mw	0	0	0	100	90	160
Load, Mvar	0	0	0	70	30	110
x_d, x'_d, x_q	0.8, 0.8, 0.2	1.3, 1.3, 0.15	0.9, 0.9, 0.25			
T_{do}	9	5.8	6			
H	20	4	5			
K_e, T_e	25, 0.05	25, 0.05	25, 0.05			

Then the MJS model parameters can be formulated as:

$$A_1 = \begin{bmatrix} 0.944 & 11.1 & -0.05787 & 0.001922 & 0.007303 & 0.0007488 \\ -0.00979 & 0.944 & -0.01009 & 0.0003337 & 0.001922 & 0.0001276 \\ -0.01347 & -0.07725 & 0.9745 & 0.0005888 & 0.003392 & 0.0008 \\ 0.001416 & 0.005376 & 0.0006038 & 0.9677 & 11.19 & -0.0308 \\ 0.000246 & 0.001416 & 0.0001028 & -0.00568 & 0.9677 & -0.005405 \\ 0.0003515 & 0.002025 & 0.0004876 & -0.005263 & -0.02999 & 0.9862 \end{bmatrix}$$

$$A_2 = \begin{bmatrix} 0.9579 & 11.15 & -0.05094 & 0.003087 & 0.01171 & 0.0007018 \\ -0.00737 & 0.9579 & -0.008911 & 0.0005375 & 0.003087 & 0.0001183 \\ -0.008995 & -0.05142 & 0.9786 & 0.0008484 & 0.004875 & 0.001136 \\ 0.002263 & 0.008582 & 0.0003783 & 0.9677 & 11.19 & -0.03057 \\ 0.0003946 & 0.002263 & 6.222 \times 10^{-5} & -0.005671 & 0.9677 & -0.005363 \\ 0.0005322 & 0.003056 & 0.0006486 & -0.005192 & -0.02959 & 0.9862 \end{bmatrix}$$

$$A_3 = \begin{bmatrix} 0.9453 & 11.1 & -0.05691 & 0.005537 & 0.02101 & 6.213 \times 10^{-5} \\ -0.009559 & 0.9453 & -0.009927 & 0.0009633 & 0.005537 & 4.019 \times 10^{-6} \\ -0.01292 & -0.07407 & 0.9747 & 0.001621 & 0.00932 & 0.001494 \\ 0.004086 & 0.0155 & 0.001388 & 0.9765 & 11.22 & -0.02559 \\ 0.0007118 & 0.004086 & 0.0002356 & -0.004129 & 0.9765 & -0.004498 \\ 0.0007333 & 0.00422 & 0.001123 & -0.002941 & -0.01673 & 0.9888 \end{bmatrix}$$

$$B_1 = \begin{bmatrix} -0.0001004 & -2.647 \times 10^{-5} & 0.005105 & 1.057 \times 10^{-6} & 2.761 \times 10^{-7} & 1.28 \times 10^{-6} \\ 1.268 \times 10^{-6} & 3.311 \times 10^{-7} & 2.026 \times 10^{-6} & -5.152 \times 10^{-5} & -1.362 \times 10^{-5} & 0.004966 \end{bmatrix}^T$$

$$B_2 = \begin{bmatrix} -8.823 \times 10^{-5} & -2.329 \times 10^{-5} & 0.005116 & 6.714 \times 10^{-7} & 1.73 \times 10^{-7} & 1.7 \times 10^{-6} \\ 1.194 \times 10^{-6} & 3.103 \times 10^{-7} & 2.87 \times 10^{-6} & -5.113 \times 10^{-5} & -1.352 \times 10^{-5} & 0.004966 \end{bmatrix}^T$$

$$B_3 = \begin{bmatrix} -9.869 \times 10^{-5} & -2.602 \times 10^{-5} & 0.005106 & 2.434 \times 10^{-6} & 6.349 \times 10^{-7} & 2.942 \times 10^{-6} \\ 1.324 \times 10^{-7} & 2.747 \times 10^{-8} & 3.778 \times 10^{-6} & -4.276 \times 10^{-5} & -1.131 \times 10^{-5} & 0.004973 \end{bmatrix}^T$$

$$B_{w1} = B_{w2} = B_{w3} = [0.3962 \quad -5.419 \quad 0.3962 \quad -5.419 \quad 0.7924 \quad -2.5971]^T, C_1 = C_2 = C_3 = [0 \quad 1 \quad 0 \quad 1 \quad 1 \quad 0]$$

$$D_{w1} = D_{w2} = D_{w3} = 0.5$$

The transition probability matrix of this large-scale system is $\Pi = \begin{bmatrix} 0.07 & 0.005 & 0.925 \\ 0.005 & 0.07 & 0.925 \\ 0.16 & 0.16 & 0.64 \end{bmatrix}$, which is

derived based on historical data. Then the state feedback controller of MJS can be obtained according to the Lyapunov stabilization condition and the divided Kalman gain is given as follows:

$$K_1 = \begin{bmatrix} -26.0807 & -403.1869 & -321.5759 & -0.2517 & -1.2317 & -0.1667 \\ 12.9795 & -389.3460 & -383.7444 & -15.9230 & -309.7199 & -243.2505 \end{bmatrix}$$

$$K_2 = \begin{bmatrix} -27.6642 & -380.6255 & -286.6292 & -0.3613 & -1.2850 & 3.5684 \\ -2.3097 & -11.5522 & 156.1355 & -30.1964 & -390.8614 & -157.0249 \end{bmatrix}$$

$$K_3 = \begin{bmatrix} -26.3066 & -379.9751 & -297.4265 & -0.7193 & -3.3943 & -0.2490 \\ -11.9466 & -230.2617 & -264.3213 & -44.8940 & -552.8994 & -312.8214 \end{bmatrix}$$

The estimation result of each state component is provided in Fig. 10. In this figure, it can be found that periodic oscillations occurred in the state components, which is more complicated than that in the SMIB instance. Then the estimation result of the KF framework based on the derandomization technique, the subsystems and weighted expectation are provided. Obviously, even the absolute value of the state component varies in a large range. The proposed technique can help the KF framework track the real state as well, which clearly exhibits the effectiveness and priority of the proposed technique. For better understanding, Table 7 provides the RMSE of the estimation result in the large-scale power system. From the estimation result figure and the error table, the estimation tracks the real state, but the estimation error is different. Mostly, the state components have the lowest estimation error except x_4 with the help of KF based on the derandomization technique.

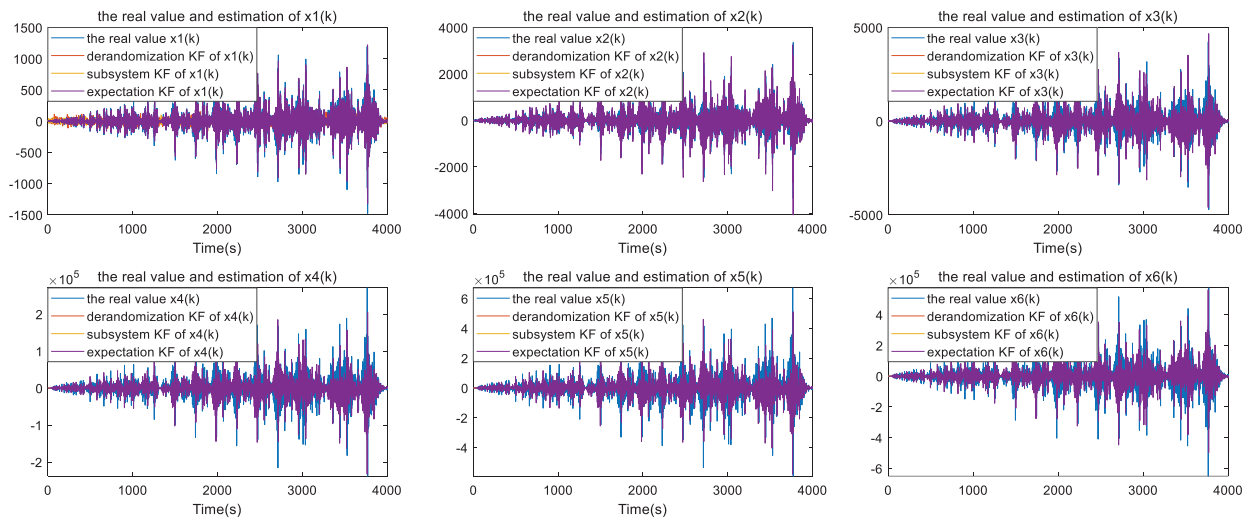


Figure 10: The estimation result and the real value of each state component in a large-scale system

Table 7: RMSE of different state components in a large-scale system

State component	Derandomization KF	Expectation KF	Robust KF
x_1	8.4235	13.6736	12.4330
x_2	0.2645	0.8001	1.1210
x_3	0.5304	1.1842	1.2920
x_4	3.7019	1.0199	1.4631
x_5	0.3168	0.7845	1.4749
x_6	0.2979	1.0221	0.6563

From the above simulation results, it can be found that this proposed method has the potential to be applied in the multi-machine cases, like 6-bus and 3-machine. However, it must also be admitted that when this method is applied to large-scale power grids, there will be a curse of dimensionality, that is, by randomizing the m-mode MJS into a single mode system, but the state dimension will rapidly expand,

requiring high solving ability. It should be noted that by aggregating equivalent circuits of large-scale power grids, the dimension of the state matrix can be reduced, so this method still has certain generalizability.

5 Conclusions

This paper proposes a recursive state estimation algorithm based on derandomization for Markov Jump Systems (MJSs) in power system applications. The power system with random abrupt changes is first modeled as an MJS, considering stochastic mode transitions governed by a Markov process. Using derandomization, the MJS is transformed into an equivalent deterministic system while preserving the state norm. A recursive estimation algorithm is then developed based on this transformed system. For comparison, existing Kalman filtering methods for MJSs are also revealed, where mode-dependent parameters are approximated as well. In the case of circuit breakers (CBs), the proposed method converts the MJS model into a single-mode system, and the Kalman filter is applied to estimate the state while accounting for stochastic switching among subsystems. Simulation results on a CB model demonstrate the effectiveness and superiority of the proposed approach over existing algorithms. Furthermore, parameter uncertainties caused by component failures are common in real-world power systems, suggesting that future work should focus on recursive state estimation under unknown or time-varying system parameters to enhance robustness in practical energy systems. Future research may attempt to develop recursive state estimation algorithms capable of handling uncertain parameters under fault conditions, thereby improving the robustness and practical applicability of estimation techniques in complex power systems. Such advancements are essential for enhancing the observability and resilience of smart grids, particularly in the presence of high renewable energy penetration and dynamic load behaviors.

Acknowledgement: Not applicable.

Funding Statement: The authors received no specific funding for this study.

Author Contributions: The authors confirm contribution to the paper as follows: Conceptualization, Quan Li and Ziheng Zhou; methodology, Ziheng Zhou; software, Ziheng Zhou; validation, Ziheng Zhou; formal analysis, Ziheng Zhou; investigation, Quan Li; resources, Quan Li; data curation, Quan Li; writing—original draft preparation, Ziheng Zhou; writing—review and editing, Ziheng Zhou; visualization, Quan Li; supervision, Quan Li; project administration, Quan Li; funding acquisition, Quan Li. All authors reviewed the results and approved the final version of the manuscript.

Availability of Data and Materials: The data that support the findings of this study are available from the Corresponding Author, Quan Li, upon reasonable request.

Ethics Approval: Not applicable.

Conflicts of Interest: The authors declare no conflicts of interest to report regarding the present study.

References

1. Anderson PM, Fouad AA. Power system control and stability. Hoboken, NJ, USA: John Wiley & Sons, Inc.; 2008.
2. Rafique Z, Khalid HM, Muyeen SM, Kamwa I. Bibliographic review on power system oscillations damping: an era of conventional grids and renewable energy integration. *Int J Electr Power Energy Syst.* 2022;136(3):107556. doi:10.1016/j.ijepes.2021.107556.
3. Khalid HM, Flitti F, Mahmoud MS, Hamdan MM, Muyeen SM, Dong ZY. Wide area monitoring system operations in modern power grids: a Median regression function-based state estimation approach towards cyber attacks. *Sustain Energy Grids Netw.* 2023;34(2):101009. doi:10.1016/j.segan.2023.101009.

4. Khalid HM, Qasaymeh MM, Muyeen SM, El Moursi MS, Foley AM, Sweidan TO, et al. WAMS operations in power grids: a track fusion-based mixture density estimation-driven grid resilient approach toward cyberattacks. *IEEE Syst J*. 2023;17(3):3950–61. doi:10.1109/JSYST.2023.3285492.
5. Nocoń A, Paszek S. A comprehensive review of power system stabilizers. *Energies*. 2023;16(4):1945. doi:10.3390/en16041945.
6. India SU, Kumar A, Akbar Hussain DM, Denmark AU. HVDC (high voltage direct current) transmission system: a review paper. *Gyancity J Eng Technol*. 2018;4(2):1–10. doi:10.21058/gjet.2018.42001.
7. Mahmud SU, Nahid-Al-Masood. Performance comparison between synchronous condenser and static VAR compensator to improve system strength in a wind dominated power grid. In: 2020 11th International Conference on Electrical and Computer Engineering (ICECE); 2020 Dec 17–19; Dhaka, Bangladesh. doi:10.1109/icece51571.2020.9393153.
8. Hatziaargyriou N, Milanovic J, Rahmann C, Ajarapu V, Canizares C, Erlich I, et al. Definition and classification of power system stability-revisited & extended. *IEEE Trans Power Syst*. 2021;36(4):3271–81. doi:10.1109/TPWRS.2020.3041774.
9. Zhang G, Hu W, Cao D, Huang Q, Yi J, Chen Z, et al. Deep reinforcement learning-based approach for proportional resonance power system stabilizer to prevent ultra-low-frequency oscillations. *IEEE Trans Smart Grid*. 2020;11(6):5260–72. doi:10.1109/TSG.2020.2997790.
10. Kim JJ, Park JH. A novel structure of a power system stabilizer for microgrids. *Energies*. 2021;14(4):905. doi:10.3390/en14040905.
11. Peyghami S, Blaabjerg F, Palensky P. Incorporating power electronic converters reliability into modern power system reliability analysis. *IEEE J Emerg Sel Top Power Electron*. 2021;9(2):1668–81. doi:10.1109/jestpe.2020.2967216.
12. Afzal S, Mokhlis H, Illias HA, Mansor NN, Shareef H. State-of-the-art review on power system resilience and assessment techniques. *IET Generation Trans Dist*. 2020;14(25):6107–21. doi:10.1049/iet-gtd.2020.0531.
13. Bhusal N, Abdelmalak M, Kamruzzaman M, Benidris M. Power system resilience: current practices, challenges, and future directions. *IEEE Access*. 2020;8:18064–86. doi:10.1109/access.2020.2968586.
14. Bahmani MH, Esmaeili Shayan M, Fioriti D. Assessing electric vehicles behavior in power networks: a non-stationary discrete Markov chain approach. *Electr Power Syst Res*. 2024;229(1):110106. doi:10.1016/j.epsr.2023.110106.
15. Han X, Wei Z, Hong Z, Zhao S. Ordered charge control considering the uncertainty of charging load of electric vehicles based on Markov chain. *Renew Energy*. 2020;161(2):419–34. doi:10.1016/j.renene.2020.07.013.
16. Kuppusamy S, Joo YH, Kim HS. Asynchronous control for discrete-time hidden Markov jump power systems. *IEEE Trans Cybern*. 2021;52(9):9943–8. doi:10.1109/tcyb.2021.3062672.
17. Borisov A, Sokolov I. Optimal filtering of Markov jump processes given observations with state-dependent noises: exact solution and stable numerical schemes. *Mathematics*. 2020;8(4):506. doi:10.3390/math8040506.
18. Zhang W, Natarajan B. On the performance of Kalman filter for Markov jump linear systems with mode mismatch. *Circuits Syst Signal Process*. 2021;40(4):1720–42. doi:10.1007/s00034-020-01545-0.
19. Costa OLV, de Oliveira AM. Filtering for nonlinear and linear Markov jump systems. *IEEE Trans Autom Control*. 2024;69(5):3309–16. doi:10.1109/TAC.2023.3322379.
20. Wan H, Karimi HR, Luan X, Liu F. A self-triggered control scheme for Markov jump systems under multiple range performance restrictions. *IFAC-PapersOnLine*. 2020;53(2):2783–8. doi:10.1016/j.ifacol.2020.12.938.
21. Allagui A, Elwakil AS. On the theory and application of the fractional-order Dirac-delta function. *IEEE Trans Circuits Syst II Express Briefs*. 2024;71(3):1461–5. doi:10.1109/TCSII.2023.3324702.
22. Soliman H, Shafiq M. Robust stabilisation of power systems with random abrupt changes. *IET Generation Trans Dist*. 2015;9(15):2159–66. doi:10.1049/iet-gtd.2014.1111.
23. Kaviarasan B, Sakthivel R, Kwon OM. Robust fault-tolerant control for power systems against mixed actuator failures. *Nonlinear Anal Hybrid Syst*. 2016;22:249–61. doi:10.1016/j.nahs.2016.05.003.
24. Qi C, Li Y, Bao J, Zhu M. Convergence analysis of the factorial Kalman filter. *IEEE Signal Process Lett*. 2025;32:2249–53. doi:10.1109/lsp.2025.3567424.

25. Dahan Y, Revach G, Dunik J, Shlezinger N. Bayesian KalmanNet: quantifying uncertainty in deep learning augmented Kalman filter. *IEEE Trans Signal Process.* 2025;73:2558–73. doi:10.1109/tsp.2025.3581703.
26. Zhao X, Mu D, Gao Z, Zhang J, Li G. Stochastic stability of the improved maximum correntropy Kalman filter against non-Gaussian noises. *Int J Control Autom Syst.* 2024;22(3):731–43. doi:10.1007/s12555-021-1119-4.
27. Zhang Y, Wang H, Zheng J, Hua L, Zhang R, Xie J. Localization and ambiguity resolution algorithm for time-difference fusion of three satellites based on observation filtering. *Sci Rep.* 2025;15(1):26060. doi:10.1038/s41598-025-10236-2.